NISTIR 6588

FIFTEENTH MEETING OF THE UJNR PANEL ON FIRE RESEARCH AND SAFETY MARCH 1-7, 2000

VOLUME 1

Sheilda L. Bryner, Editor

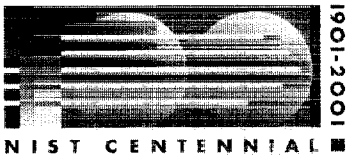

National Institute of Standards and Technology
Technology Administration, U.S. Department of Commerce

NISTIR 6588

FIFTEENTH MEETING OF THE UJNR PANEL ON FIRE RESEARCH AND SAFETY MARCH 1-7, 2000

VOLUME 1

Sheilda L. Bryner, Editor

November 2000

U. S. Department of Commerce
Norman Y. Mineta, Secretary
Technology Administration
Dr. Cheryl L. Shavers, Under Secretary of Commerce for Technology
National Institute of Standards and Technology
Raymond G. Kammer, Director

Suppression of Low Strain Rate Flames by an Agent

Anthony Hamins, Matthew Bundy and Ishwar Puri*
BFRL, NIST, Gaithersburg, Maryland 20899-8640
*Dept. Mechanical Engineering, University of Illinois at Chicago, Chicago, Illinois 60607-7022

Abstract

The structure and suppression of low strain rate methane-air nonpremixed flames were investigated experimentally and computationally. Measurements of the critical suppression conditions were conducted using N_2, CO_2, and CF_3Br added to the fuel or oxidizer streams. Temperature measurements were made with small platinum thermocouples (0.025 mm wire diameter) that were coated with a fine layer (0.010 mm) of SiO_2 and corrected for radiative losses. Numerical simulations of the non-luminous diluted flames included radiative heat losses by participating gaseous species. A previously developed narrowband model of radiative transfer was incorporated into the one-dimensional flame simulation. For comparison, radiation was also modeled as an optically thin gray gas, represented by Plank mean absorption coefficients.

Introduction

The agent concentration required to achieve the suppression of low strain rate nonpremixed flames is an important consideration for fire protection in a microgravity environment such as a space platform. Currently, there is a lack of understanding of the structure and energetics associated with the suppression of low strain rate ($<20\ s^{-1}$) nonpremixed flames, as well as the suppression effectiveness of agents in these flames [1]. The exception to this statement is the study by Maruta et al. [2], who reported measurements of low strain rate ($a_g = 2\ s^{-1}$ to $15\ s^{-1}$) suppression of methane-air diffusion flames with N_2 added to the fuel stream under microgravity conditions. They found that the nitrogen concentration required to achieve extinction increased as the strain rate decreased until a critical value ($7\ s^{-1}$) was obtained. As the strain rate was further decreased, the required N_2 concentration decreased. This behavior was attributed to radiation-induced nonpremixed flame extinction. In terms of fire safety, the existence of a critical maximum value of agent concentration required for flame extinction represents a fundamental limit.

Agent suppression requirements of low strain rate counterflow flames are also important because they correspond to the agent suppression requirements in buoyancy dominated coflowing flames, such as cup burner flames. Counterflow flames are a convenient configuration for control of the flame strain rate. In high and moderately strained near-extinction nonpremixed flames, analysis of flame structure typically neglects radiant energy loss because the flames are nonluminous and the hot gas species are confined to a thin reaction zone where they are insufficient to cause significant radiative emission. For example, in counterflowing methane-air nonpremixed flames, radiative heat loss fractions with values ranging from 1 to 6 percent have been predicted and measured [3,4].

The objective of this investigation is to answer the following questions. (1) To what extent does radiation heat loss impact the extinction of a nonpremixed flame by an agent? (2) At

what strain rate does radiative loss become significant? Here, we report progress on answering these questions, as the competing processes of thermal radiation, flame stretch, and agent addition that lead to flame extinction are investigated. Measurements of flame structure and extinction were compared with simulations that included radiative heat transfer. In the experiments, a suppressant (N2, CO_2, or CF_3Br) was added to either the fuel stream or oxidizer stream of methane-air diffusion flames. These agents were considered because N_2 is an inert species that simplifies the interpretation of experimental results, CO_2 is a common fire suppressant, and CF_3Br represents a baseline for chemically acting agents.

Experimental Method

Experiments were conducted using a water-cooled counterflow burner with a diameter of 23.4 mm and a duct separation of 25 mm. Four 200 mesh stainless steel screens were secured at the opening of each duct to impose a top-hat velocity profile. The flow of dry air and methane (99.99% pure) were controlled using mass flow controllers that were calibrated using a dry cell primary flow meter with an uncertainty of better than 0.5%. The ratio of the velocity of the oxidizer stream to the velocity of the fuel stream was controlled (typically 3:1) to position the flame such that conductive heat transfer losses to the burner were eliminated, as verified by temperature measurements using thermocouples.

Extinction measurements were performed by incrementally increasing the agent flow, while maintaining a constant global strain rate, accomplished by simultaneously reducing the air or fuel flow. The global strain rate (a_g) was varied from approximately 8 s^{-1} to 45 s^{-1}, where for sake of comparison with Ref. [2], the global strain [5,6] is defined here as:

$$a_g = (-V_O/L)\cdot(1 + [V_F(\rho_F)^{1/2}/(-V_O(\rho_O)^{1/2})])$$

The parameters V and ρ denote the velocity and density of the reactant streams at the boundaries, L is the duct separation distance, and the subscripts O and F represent the oxidizer and fuel streams, respectively. Extinction measurements were repeated at least four times. The combined standard uncertainty (with a coverage factor of 2, i.e., k=2) in the agent extinction concentration based on repeat measurements and a propagation of error analysis was 1.3%.

In this study, flame unsteadiness was reduced by placing the burner in an enclosure ($0.5\times0.5\times0.6$ m^3), which isolated it from ambient flow disturbances and facilitated experimentation on flames with global strain rates (a_g) as low as 8 s^{-1}. The enclosure had a 10 cm exhaust port, with ventilation forced by a small pressure differential. For experiments involving CF_3Br, the enclosure was placed inside of a chemical hood.

Temperature measurements were conducted using 0.025 mm (0.001") diameter (Pt/Pt + 10%Rh) S-type thermocouples coated with a thin (0.01 mm) layer of silica. The thermocouple wires were oriented horizontally along an isotherm to minimize conductive losses. A small thermocouple was used to minimize the radiation correction to the temperature measurement and to minimize flame destabilization. This effect was quantified by measuring the N_2 concentration required to achieve extinction with the thermocouple at the position of peak temperature. The thermocouple presence cooled the flame 10 K and reduced the flame enthalpy by <0.5%. Radiation correction to the temperature measurements were made assuming a spherical bead shape using Ranz and Marshall's correlation for Nusselt number as described in Ref. [7], while the local Reynolds number was determined from the flame structure calculations. The emissivity

of the SiO_2 coating (ε =0.22±0.02) was taken from Kaskan [8]. The radiation correction was 40 K at T≈1600 K, and was insensitive to the local velocity. The combined standard uncertainty (k=2) in the temperature measurement based on repeated measurements and a propagation of error analysis was 30 K, a value dominated by measurement variation.

Numerical Methodology

Numerical simulations of strained atmospheric methane-air flames were performed using a previously developed computer code [9] that employs detailed models of molecular transport and chemistry [10]. The use of counterflow codes to model inhibited nonpremixed flames is now routine, and the methodology is explained in detail elsewhere [3,11]. The agents considered in the simulations, N_2 and CO_2, are chemically inert, but the latter participates both as an emitter and an absorber in radiative transfer. The counterflow code does not include a buoyancy term in the momentum equation, so the simulations represent zero gravity conditions. A multi-dimensional code that accounts for buoyancy is being developed.

A term for the radiative heat loss rate per unit volume was added to the energy equation in the one-dimensional flame code [9]. Thermal radiation was modeled two ways. The temperature-dependent Planck mean absorption coefficients for participating gas species (CH_4, CO_2, H_2O, and CO) were obtained from Ref. [12]. A previously developed narrowband model for combustion-related radiation calculations was also implemented [13]. The mixture absorption coefficient for each isothermal layer (assumed semi-infinite) was calculated using the narrowband model, which uses a combination of tabulated data and theoretical approximations. The narrowband model calculates the radiative flux from a volume containing variable partial pressures of participating species (CH_4, CO_2, H_2O, and CO) [13]. The total directed radiated energy flux from the domain and its spectral distribution were calculated. The calculation implicitly assumes that radiative transfer occurs in the axial direction, which is consistent with the measurements of Lee et al. [3], who showed that the axial radiative flux is approximately six times greater than that emitted in the transverse direction. The value of the total flame heat release rate, Q, was quantified by summing the local heat release per unit volume (with contributions from each chemical reaction) and integrating this along the central axis of the domain. The radiative fraction is defined as: $\chi_R = Q_R/Q$.

Results and Discussion

Observations

Undiluted, low strain rate counterflow methane-air flames are luminous. As either CO_2 or N_2 was added to the oxidizer or fuel streams, flame luminosity decreased until, near extinction, the flames appeared to be completely nonluminous. (This was also observed for acetylene, a fuel that is extremely smoky under undiluted conditions.) The high inert content in the flames produces relatively cool temperatures, which precludes the formation of particulates that are otherwise present in the low strain flames. This observation motivated simplification of the radiation model for flames with CO_2 and N_2 added, permitting exclusion of radiative emission by particulate. This was not the case for CF_3Br, which when added to the methane-air flame, yielded a very luminous flame.

Suppressant added to the Fuel Stream

Figure 1 shows the measured N_2, CO_2, and CF_3Br concentrations in the oxidizer stream as a function of the global strain rate required for suppression. The most effective suppressant (on a volume basis) was CF_3Br, followed by CO_2 and then N_2. The critical suppressant concentration increased as the strain rate decreased, with the values leveling off near 15 s^{-1}, except for CF_3Br, which exhibited a turning point near 20 s^{-1}.

Figure 2 compares our measurements and calculations with the microgravity measurements of Maruta et al. and their numerical results, which were based on an optically thin gas assumption and an imposed duct separation distance of 8 cm. The experimental result from Refs. [6,14] are also shown, as are our simulations using both the narrowband and optically thin models corresponding to the conditions defined in Table 1 of Ref. 2. The three sets of calculations shown in Fig. 2 follow a gross trend similar to the measurements, but deviate from the measurements (and each other) at strain rates below 20 s^{-1}. The narrowband simulations predict that the fundamental limit occurs at a N_2 mole fraction, $[N_2]$, of 0.89 (a_g = 2.3 s^{-1}), which is lower than the prediction based on the optically thin assumption, $[N_2]$ = 0.88. This is expected, since the optically thin model does not consider reabsorption, and thus over-predicts radiative loss. The inclusion of reabsorption increases flame stability, similar to premixed flames [15]. At higher strains, radiation effects are less prominent and differences between the radiation models are less significant. The microgravity experiments from Ref. [2] were replicated in normal gravity, until the flames became unsteady for a_g <13s^{-1}, precluding confirmation of the turning point behavior for N_2 (see Fig. 2).

Suppressant added to the Oxidizer Stream

Figure 3 shows the measured concentrations of N_2, CO_2, and CF_3Br as a function of the global strain rate for agent added to the oxidizer stream. Consistent with Fig. 1, the most effective suppressant was CF_3Br, followed by CO_2 and then N_2. Flames with N_2 and CF_3Br addition showed turning point behavior at 20 s^{-1} and 15 s^{-1}, respectively. This was somewhat lower than observed when CF_3Br was added to the fuel stream (see Fig. 1), which may be due to differences in radiative emission, indicated by higher luminosity in the flames with fuel side CF_3Br addition.

The strain rate has a strong influence on flame stability. Figure 4 shows the calculated and measured concentration of CO_2 in the oxidizer stream required to extinguish the methane/air flames as a function of the global strain rate (a_g). The calculated and measured concentrations of CO_2 are in agreement, increasing as a_g decreases. At small strain rates, radiative heat losses are relatively more significant and consequently the amount of CO_2 required for suppression is lower than for the nonradiating flame case. Also shown in Fig. 4 are the calculated and measured maximum temperatures in the flames. The measured maximum flame temperatures decrease with decreasing strain rate, in agreement with the calculated trends. The flames also become spatially broader as the strain decreases. Differences in the absolute value between measurements and calculations are within 40 K, attributed to experimental uncertainty.

At a specified value of a_g, the calculated near-suppression maximum flame temperatures are nearly identical for all three radiation models. This suggests that regardless of the enthalpy loss mechanism, whether by thermal radiation or a combination of sensible heat extraction and

CO_2 dilution, the flames extinguish at nearly the same maximum temperature. This is in accord with the theory of flame extinction that holds that extinguishment occurs when heat losses are greater than heat production, independent of the mechanism.

At moderate strain rates (~50 s^{-1}), there is a negligible difference in the [CO_2] required for extinguishment using the three radiation treatments (Planck mean/optically thin, the narrowband model, and assuming adiabatic conditions, effectively ignoring radiative loss). At lower strain rates, however, as the relative importance of the radiation losses becomes significant, the agent required to extinguish a radiating flame is significantly lower that needed to extinguish a non-radiating flame. Because the narrowband model accounts for reabsorption of thermal radiation, there are lower enthalpy losses than the optically thin model and consequently the flames are more robust and require higher agent concentrations for extinguishment. Calculations yield $\chi_R = 0.010, 0.015, 0.028, 0.075$ for strain rates of 52 s^{-1}, 34 s^{-1}, 17 s^{-1}, and 5.7 s^{-1}, respectively. Even at very low strain rates, radiative loss accounts for only a small fraction of the flame heat loss, consistent with the results for N_2 addition flames [2].

Summary and Conclusions

The structure and suppression of methane-air diffusion flames was investigated through experiments and simulations. The competing processes of thermal radiation, flame stretch, and agent addition were characterized.

- The range of global strain rates investigated in normal gravity can be extended by isolating the burner in order to reduce disturbances by ambient currents, and by varying the velocity ratio of fuel and oxidizer to minimize conductive losses to the burner. Turning point behavior, where the agent concentration obtains a limiting value insuring suppression under all conditions, was observed in normal gravity diffusion flames.
- Diluted, low strain rate hydrocarbon-air flames are nonluminous near-suppression, which simplifies the treatment of radiation heat transfer in the calculation of flame structure. Flames with CF_3Br are luminous and particulate contributions to radiative emission should be considered.
- Flame structure calculations show that as the strain rate decreases, the flames broaden. Flame stability, as exemplified by agent concentration requirements for suppression, increases as the strain rate decreases, yet the peak flame temperature is found to decrease, both computationally and experimentally.
- Although the agent suppression requirements varied, the calculated peak flame temperature at suppression was the same when the radiation was treated as either optically thin, narrowband, or adiabatic, indicating that the flame temperature is independent of the heat loss mechanism.
- When radiative losses become significant, both the optically thin and narrowband models indicate that a limiting agent concentration (or turning point) occurs, whereas the non-radiating flame does not. Without a competing loss mechanism, the non-radiating flame continues to become more stable as its structure becomes broader. When radiative losses

become important, however, both convection and conduction losses compete with radiative losses, and flame stability no longer monotonically increases with decreasing strain rate.

Acknowledgements

This research was supported by the NASA Microgravity Research Division through Contract No. C–32066–T (NIST) and Grant No. NCC3–694 (UIC), with Dr. Sandra L. Olson serving as Technical Monitor.

References

1. Hamins, A., Trees, D., Seshadri, K., & Chelliah, H., *Combust. Flame*, 99:221 (1994).
2. Maruta, K., Yoshida, M., Guo, H., Ju, Y., & Niioka, T, *Combust. Flame*, 112:181 (1998).
3. Lee, K. Y., Cha, D. J., Hamins, A., & Puri, I. K., *Combust. Flame* 104:27 (1996).
4. Chan, S. H., Pan, X. C., & Abou-Ellail, M. M. M., *Combust. Flame,* 102:438 (1995).
5. Seshadri, K., & Williams, F.A., *Int. J. Heat Mass Transfer,* 21:251 (1978).
6. Puri, I. K., & Seshadri, K., *Combust. Flame*, 65:137-150 (1986).
7. Shaddix, C.R., "Correcting Thermocouple Measurements for Radiation Loss", Proceedings of the 33rd National Heat Transfer Conference, Albuquerque, NM, 1999.
8. Kaskan, W.E., *Sixth Symposium (International) on Combustion*, The Combustion Institute, Pittsburgh, 1957, pp. 134-141.
9. Lutz, A., Kee, R. J., Grcar, J., & Rupley, F. M., "A Fortran Program Computing Opposed Flow Diffusion Flames", SAND96-8243, Sandia National Labs, Livermore (1997).
10. Bowman, C. T., Hanson, R. K., Davidson, D. F., Gardiner, Jr., W. C., Lissianski, V., Smith, G. P., Golden, D. M., Frenklach, M., & Goldenberg, M., "GRI-MECH 2.11", URL: http://www.me.berkeley.edu/gri-mech/, 1995.
11. Yang, M. H., Hamins, A. & Puri, I. K., *Combust. Flame* 98:107-122 (1994).
12. Tien, C. L., Thermal Radiation Properties of Gases in *Advances in Heat Transfer* (T. F. Irvine Jr. and J. P. Hartnett, Eds.), Vol. 5, 1968, p. 311.
13. Grosshandler, W. L., RADCAL: NIST Technical Note 1402, National Institute of Standards and Technology, Gaithersburg, Maryland, 1993.
14. Ishizuka, S., & Tsuji, H., *Eighteenth Symposium (International) on Combustion*, The Combustion Institute, Pittsburgh, 1980, pp. 695–703.
15. Ju, Y., Masuya, G., & Ronney, P. D., *Twenty-seventh Symposium (International) on Combustion,* The Combustion Institute, Pittsburgh, 1998, pp. 2619-2626.

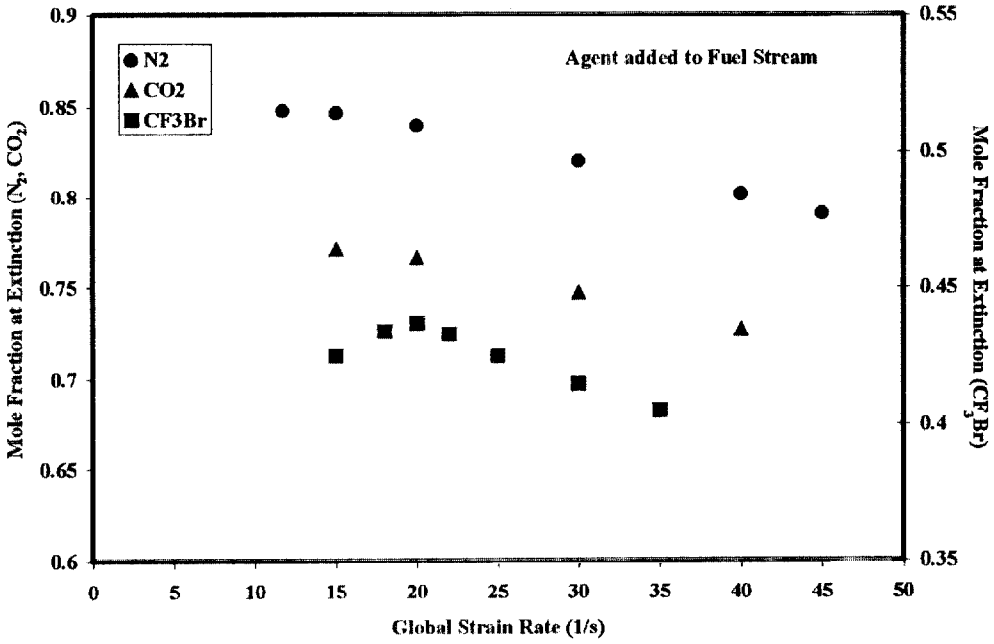

Figure 1. Measurement of the critical mole fraction of N_2, CO_2, and CF_3Br in the fuel stream of methane-air diffusion flames.

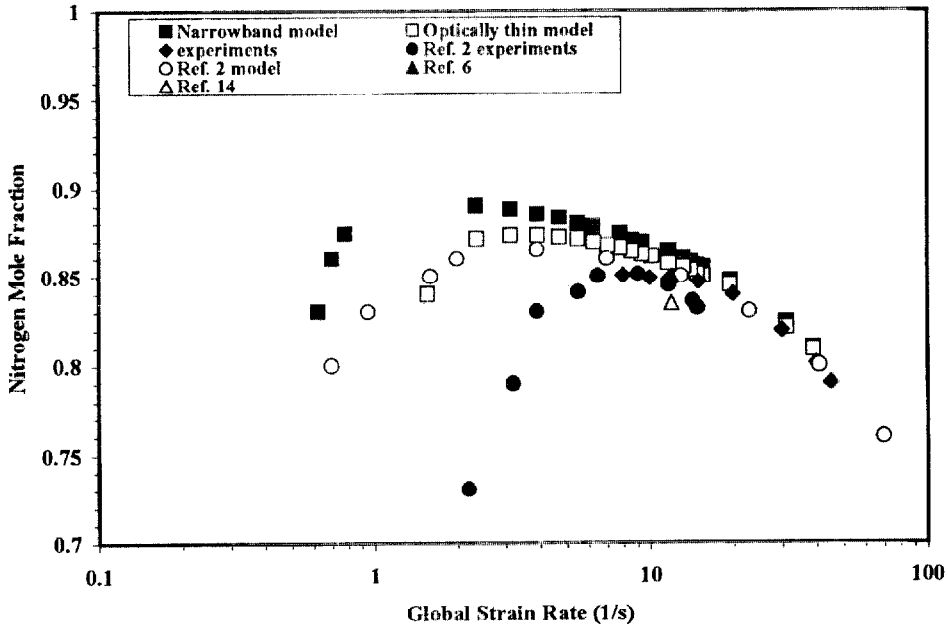

Figure 2. Comparison of measurements and simulations of the critical mole fraction of N_2 in the fuel stream of methane-air diffusion flames.

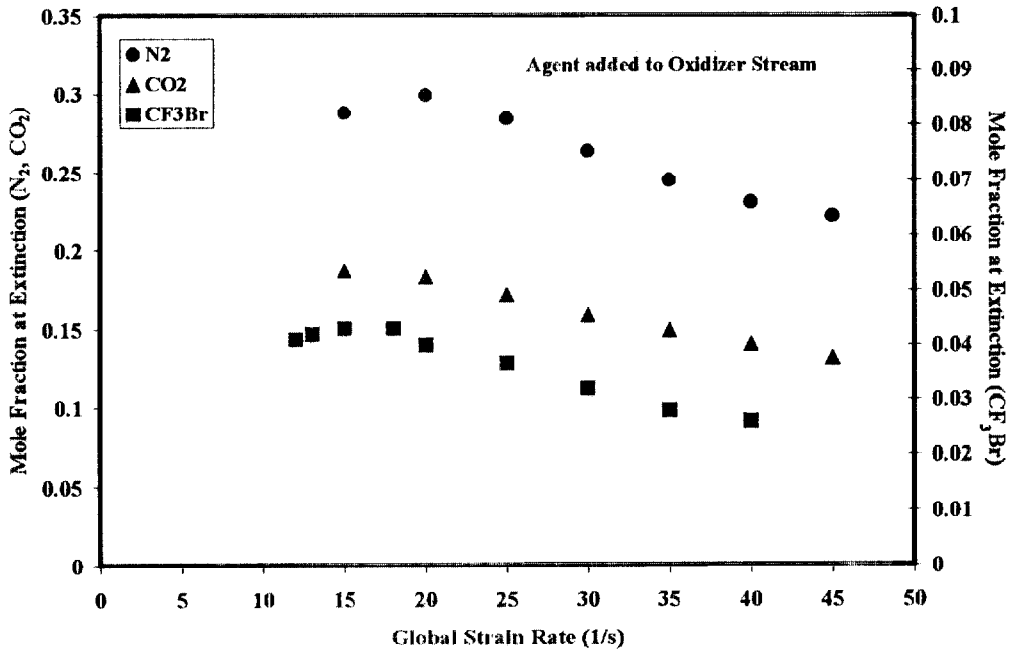

Figure 3. Measurement of the critical mole fraction of N_2, CO_2, and CF_3Br in the oxidizer stream of methane-air diffusion flames.

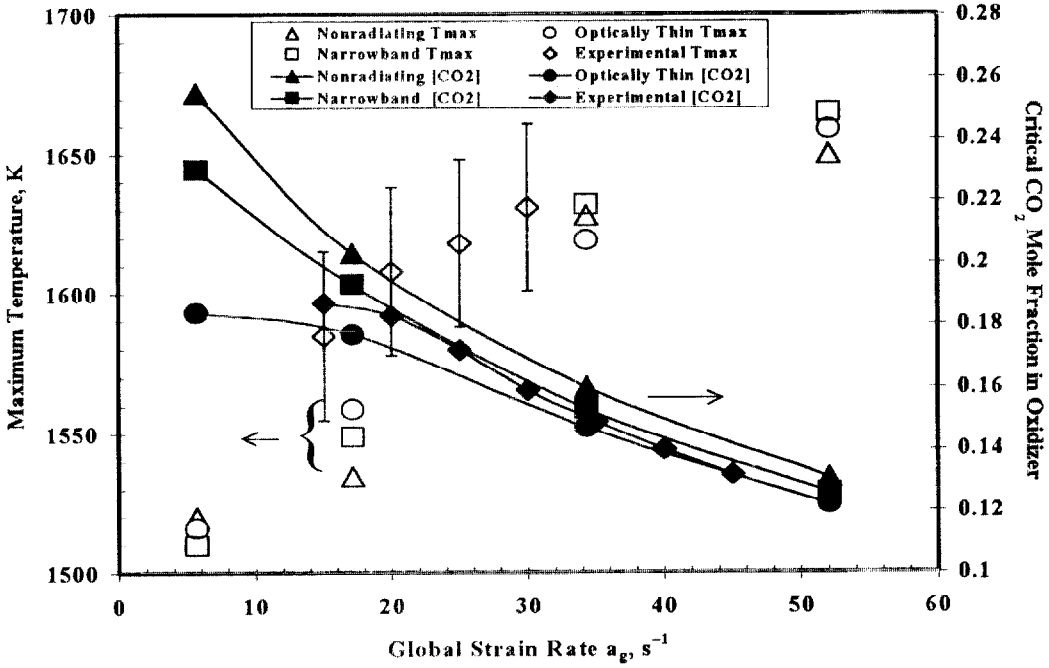

Figure 4. Comparison of measurements and simulations of the peak flame temperature and the critical mole fraction of CO_2 in methane-air diffusion flames with CO_2 added to the oxidizer stream.